Influence of arousal state on encoding of visual stimuli by neuronal populations in primary visual cortex

Bachelor Thesis

Stephan Grzelkowski,

In partial fulfillment of Bachelor of Science Psychobiology

Faculty of Science

University of Amsterdam

Student Number: 10342931

Supervision: Guido Meijer and Carien Lansink

Swammerdam Institute for Life Sciences, Cognitive and Systems Neuroscience Group

19.07.2016, Amsterdam

Abstract

Arousal affects the cortical mechanisms of information encoding, influencing the way an organism processes the stimuli in its surroundings. Complex tasks show best performance at intermediate levels of arousal, the optimal state. Although recent studies have looked at several neuronal correlates of different states of arousal, most classify arousal in two distinct states. Since optimal state of arousal is observed at intermediate levels, which is not considered when discriminating between two states, the neuronal correlates of arousal at optimal level are not well understood. The effect of optimal state of arousal on population coding in the primary visual cortex was investigated using two-photon calcium imaging in awake and behaving mice. These measurements were combined with eye-tracking of the pupil of the mouse as a measurement of arousal. Earlier results of a u shaped curve of activity and variability to levels of arousal in the mouse auditory cortex were replicated in the visual cortex. Noise correlations are a mechanism shown to be involved in sensory processing. We found noise correlations to be increased at high pupil sizes compared to low and intermediate levels. More interestingly we also observed a significant decrease of noise correlation at optimal state of arousal comparing hit against miss trials. These results implicate that a decorrelation of the activity of neurons have a positive effect on information encoding. Our findings suggest a neuronal basis for optimal task performance at intermediate levels of arousal.

Introduction

Arousal optimizes the way the cortex processes information in different situations. When looking at the mouse as a model organism one can imagine that at low levels of arousal the mouse is in a state of relaxation and it is not required for the mouse to be attentive to its surroundings. Intermediate levels of arousal are optimal for task solving for which sensory processing is likewise required to be at its optimum. High levels of arousal in turn are linked to threatening situations, where the mouse is in a state of fight-or-flight and relies on reflexes whereby sensory processing is of less importance. These finding have been described in the Yerkes-and-Dodson-law. Optimal task performance occurs at moderate levels of arousal, where decreases in task performance are caused by a lack of attention or high anxiety at low and high levels of arousal respectively (Yerkes and Dodson, 1908). These results are numerously replicated in humans, primates and rodents. However, the neural correlates of the optimal state of arousal for sensory processing are largely unknown.

The mouse cortex is a popular target for research investigating the neuronal mechanisms of sensory processing on a cellular and population level. A multitude of studies examined the effects of arousal on information encoding in different modalities. They consistently report improvements on sensory processing in states associated with high arousal (Ecker et al., 2014; Reimer et al., 2014; Vinck et al., 2015). Most studies take to a binary classification of states, discriminating only between states of high and low arousal. This is, however, a significant shortcoming considering that optimal task performance is reported at intermediate levels of arousal, therefore negated in these cases. Recent work in the auditory cortex of the mouse used a continuous approach in the evaluation of state of arousal. Subthreshold membrane potential showed a u-shaped interaction with arousal with a minimum at intermediate arousal levels. Auditory evoked activity measured in the firing rate of Layer IV/V neurons in the auditory cortex showed peaks at intermediate levels of arousal accompanied by a high reliability of the neuronal responses in both cases with a decrease towards high and low levels of arousal. Variability of the response was found to be a u-shaped curve in relation to the level of arousal (McGinley et al., 2015a).

Response variability of neurons in response to a stimulus is a fundamental mechanism in the encoding of sensory information. The correlations in the variability between pairs of neurons, called noise correlations, are of importance in understanding the mechanisms of population encoding. There is an ongoing discussion whether noise correlations are detrimental to population coding or that they also can have a beneficial effect. Depending on the structure of the correlations, they have been shown to be able to improve or hamper stimuli encoding (Averbeck et al., 2006; Faisal et al., 2008; Franke et al., 2016). Results from different studies conducted in the rodent visual cortex consistently show decreased noise correlations during more active states. Noise correlations are decreased during dilation of the pupil compared to constriction in V1 neurons during visual stimulations, as well as during periods long after (5-20s) locomotion compared to periods of locomotion and periods shortly after (1-5 s) locomotion, where locomotion shows increases in pupil diameter (Reimer et al., 2014; Schölvinck et al., 2015; Vinck et al.,

2015). Most studies use a binary approach when discriminating states in noise correlation analysis and do not distinguish between hit and miss trials. As the optimal state for task performance is at intermediate arousal levels these can be shortcomings that we aim to clarify. Considering the response of the animal might reveal interesting neuronal mechanisms that can be linked to the behavior of the animal.

The arousal system consists of multiple neurotransmitter systems, most importantly the dopaminergic system in the ventral tegmental area (VTA), the locus coeruleus (LC) noradrenergic group and the magnocellular basal forebrain regulating the cholinergic system. These systems innervate most cortical areas and different cortical layers (Marrocco et al., 1994). In addition, the cholinergic pathway also regulates the dilation and constriction of the pupil. Thus, pupillometry is directly correlated to the level of arousal and with the use of infrared cameras it is an accessible and non-invasive method for measurement (Beatty, 1982; Bradley et al., 2008; Zoccolan et al., 2010).

Recent studies investigated the relation of arousal and sensory encoding in the auditory cortex (McGinley et al., 2015b). To see if similar results can be obtained in a different modality, we focus on the primary visual cortex of the mouse. This leads to the question: How does optimal state of arousal shape information encoding in the primary visual cortex? In this study we aim to expand the knowledge of the interaction between different states of arousal to the primary visual cortex during a visual detection task. Furthermore, we expand the binary approach to state classification of previous studies (Ecker et al., 2014; Reimer et al., 2014; Vinck et al., 2015), by also considering intermediate levels of arousal and distinguishing between hit and miss trials, to investigate the effects on activity and variability of the neuronal response as well as noise correlations.

To measure neuronal activity, we used two-photon calcium imaging enabling simultaneous measurement of a large population of neurons in layer II/III of the primary visual cortex of the mouse (Helmchen and Denk, 2005; Stosiek et al., 2003). We found that spontaneous activity and the variability in activity in the primary visual cortex show minima at intermediate levels of arousal with increases at low and high levels of arousal forming a u-shaped curve. Noise correlations are increased at high levels of arousal compared to intermediate and low levels. When comparing the noise correlation between hit and miss trials we observed a decrease in hit trials at intermediate levels.

Materials & Methods

Animals

Tests were carried out on C57B1/6 80-216 mice according to the Dutch national guidelines on the conduct of animal experiments. They were obtained from the Harlan Sprague Dawley Inc. or from in-house breeding lines. The mice were housed in a standard enriched cage in groups of 2-4 with a 12-hour reversed light/dark cycle. At begin of the experiments the mice were between 190-200 days old.

Head bar implantation

Movement of the mice during two-photon imaging obstructs imaging quality. To restrict movement, the mice were implanted with a head bar to be head-fixated and placed into a body holder during the task. Before start of procedure the animals were injected with 0.05-0.1 mg/kg buprenorphine. During operation the mice were anesthetized with 1-2% isoflurane. The titanium head bar with an 8 mm circular window was positioned above the left visual cortex and secured with C&B superbond (Sun Medical, Japan). The skull was covered with cyanoacrylate glue (Locktite 401, Henkel, CT, USA).

Training

To be able to observe the effects of the level of arousal not only on the cortical mechanisms of information encoding but also on task performance, the mice were trained on a visual detection task. First the animals were habituated to the training environment by placing them into the test set up with a fixated head for short periods of time. After the animals were used to the training environment (typically after about 3-5 days) they were presented with the visual stimulus (see *Visual Stimulus*) paired with a milk reward. Between each consecutive stimulus there was an inter trial interval (ITI) of 3-5 s. The animal was conditioned to give a lick response by increasing the milk reward when a stimulus was coinciding with a lick response. Lick responses were detected using a custom build lick detection ray with an infrared beam. After the response rate was high enough for the animal to be considered conditioned, the mouse was trained on the visual detection task (see *Visual stimulation*). For the task the mouse had 1 s to give a lick response to the stimulus. D-prime was used as a measure of task performance:

$$\mathrm{d}' = \mathrm{norminv}(\mathrm{Hit\ rate}) - \mathrm{norminv}(\mathrm{False\ alarm\ rate})$$

Equation 1

With norminv() being the inverse of the cumulative function (Andermann et al., 2010). After D-prime was

consistently above 1.5 for 3 successive training sessions, mice were considered proficient in the task.

Sessions consisted of multiple blocks of stimulus presentation with an average of 20-40 trials with Visual trials, audio stimulation and audiovisual stimulation randomly shuffled. Audio and audiovisual trials were part of a different set of experiments and are therefore not discussed. To motivate the mice, they were put on a water rationing regime in which they could earn their daily ration of liquid by performing the task. During training the animals were placed in soundproof, darkened cages.

Visual stimulation

To obtain relevant information on the behavioral performance the visual stimulus had to be sufficiently difficult for the mice to make mistakes. Therefore, the stimulus contrast was changed using the adaptive staircase of the Psychtoolbox. All visual stimuli were presented using a 15'' TFT monitor (60 Hz) that was positioned 16 cm in front of the right eye in 45° from the midline. During training and the visual detection task the animals were presented with a circle of continuous moving bars at a temporal speed of 1 Hz and a spatial frequency of 0.05 cpd. The stimuli were presented in 3 different orientations (0°, 120° and 240°). Using a gray cosine-tempered circular cut, the influences of edge effects were eliminated. The stimulus had a diameter of 60 retinal degrees.

Intrinsic optical signal (IOS) imaging

IOS measures population activity of the cortex by projecting red light on the skull and reflected light is captured with a camera. More active areas of the brain are characterized by increased blood flow to the area, causing more light to be scattered and therefore less light to be reflected to the camera. During IOS the animals were lightly anesthetized using 0.5-0.1% isoflurane. The procedure was carried out using an 810 nm light stimulation and a CCD camera for light capturing with a 1 Hz sampling rate. For localization of the primary visual cortex the animals were presented with a visual stimulus (drifting gratings) of 8 different orientations each for 1 second with an ITI of 17s. The IOS was overlaid with an image of vasculature and analyzed in the VDAQ software (Optical Imaging Ltd).

Virus infection and craniotomy

In order to measure neuronal activity using two-photon calcium imaging, the target neurons were infected with a green fluorescent protein activated by calcium influx into the cell soma. During the operation the animals were anesthetized with 1-2% isopropanol and prior to surgery injected with 0.05-0.1 mg/kg buprenorphine. The viral construct AAV1.Syn.GCaMP6m/f.WPRE.SV40 (Penn Vector Core), carrying the GCaMP6m or GCaMP6f protein, was injected with a quantity of 200-300 nl. Injection was made through a drill hole with a glass pipet attached to a NanoJect II injector (Drummond Scientific Company) targeting a depth of 500-700 µm. After injection a craniotomy of 3mm over V1 was made and covered under a custom made double layered cover glass. The lower cover glass was fitted precisely in the craniotomy to imitate the structure of the lost skull and prevent its regrowth (Goldey et al., 2014). The upper cover glass of 5 mm diameter was attached to the skull using Locktite. The animals were left to recover for 1 week after which the experiment was started.

Two-photon calcium imaging

Two-photon calcium imaging was performed using a Leica SP5 resonant laser scanning microscope and a Spectra Physics Mai Tai High Performance Mode Locked Ti:Sapphire laser. The wavelength of the laser was 900-940 nm, using resonant mirrors resulting in a sampling frequency of 14.4 Hz (applying 2 frame averaging). Imaging depth was targeted at 140-200 µm in the primary visual cortex (Layer II/III). Emitted fluorescent was measured using a photo-multiplier tube with a 525 nm wavelength. For image capturing a 25x Leica objective was used resulting in an imaging plane of 365x365 µm.

2-photon data

Movement of the mice can result in miniscule movement of the 2-photon image frames in x-y directions. These were corrected by applying a single step discrete Fourier realignment procedure (Guizar-Sicairos et al., 2008). All neurons were selected using a semi-automatic script implemented in a MATLAB interface. After selection of cell bodies, neuropil subtraction was performed by averaging the fluorescence signal from an annulus of 2-5 µm around the soma of the neurons, excluding other neurons, and subtracted from the soma fluorescence signal. To prevent over subtraction of the neuropil signal, before subtraction the neuropil signal was multiplied by 0.7 (Chen et al., 2013). Neuron activity was quantified by the ΔF/F metric (equation 1).

$$\Delta F/F_0 = \frac{F^i - F_0}{F_0}$$

Equation 2

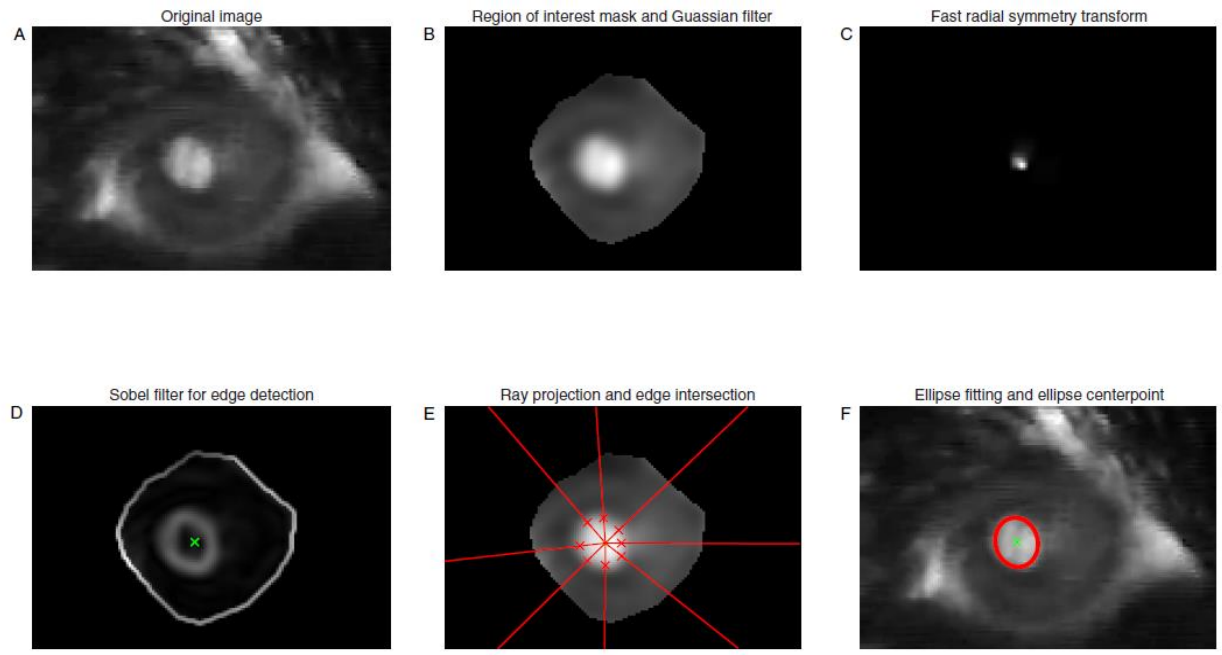

Figure 1 **Starburst algorithm implementation for Eye Tracking**
(A) Original video frame cropped using a manual assigned rectangular window (B) Applied Gaussian smoothing filter and manual region of interest mask (C) Fast radial symmetry transformed image frame with high intensity values for areas with high regional symmetry (D) Sobel filtered image. High Intensity value correspond to points with high differences in intensity to neighboring points in the original frame. Green cross marks highest intensity point of the FRST. (E) A number of rays (n = 8) projected in 8 directions with the same radial distance from one another. Red crosses mark assigned edge points for each ray. (F) The ellipse was fitted using edge points after outlier detection and displayed in red on the original frame. Green cross marks the center of the ellipse. For further details see Methods: EyeTracking

Where ΔF is the relative increase in fluorescence, F0 is baseline fluorescence and Fi is activity of the neuron at imaging frame i. F0 was calculated using a 30s sliding window before time point i as the average over all lower half fluorescence values.

Eye-Tracking

The Eye-Tracking algorithm enables non-invasive measurement of the pupil diameter of the mouse used as a quantification of the state of arousal of the animal. Video of the pupil of the mice were taken using a near-infrared camera (CV-A50 IR, JAI), that was positioned facing the ipsilateral eye relative to the stimulus presentation. The camera captured infrared light naturally emitted by the 2-photon calcium at an imaging frequency of 25 Hz. Pupil size was calculated using a custom written algorithm based on the starburst algorithm (Li et al., 2005). Every frame was cropped using a manually fitted rectangle around the eye and a region of interest masks consisting of freely connected points fitted onto the eye, decreasing the required processing power of the algorithm. The resulting frames were smoothed using a Gaussian filter algorithm. To find the center of the pupil a fast radial symmetry transform was implemented (FRST; Loy and Zelinsky, 2003) and the center point was determined as the highest value of the FRST. To find the edge of the pupil, we applied a sobel filter (*Equation 2*).

$$S_x = A * \begin{bmatrix} 1 & 0 & -1 \\ 2 & 0 & -2 \\ 1 & 0 & -1 \end{bmatrix}$$

$$S_y = A * \begin{bmatrix} 1 & 2 & 1 \\ 0 & 0 & 0 \\ -1 & -2 & -1 \end{bmatrix}$$

$$S = \sqrt{{S_x}^2 + {S_y}^2} \qquad \textit{Equation 3}$$

Where S is the filtered Image and S_x and S_y are the results of the convolution of the original image A with a horizontal and vertical direction filter respectively.

From the center we projected a number of rays (n = 16) in different directions with equal radial distance. Over the 75% of the ray-points closest to the center we evaluated the maximal value of the sobel filtered image. For outlier detection the distance of edge points to the image center were calculated and points were declared as outliers when they were 2 SD above or below average distance to center. An ellipse was fitted on the remaining edge points using an ellipse fitting algorithm written by Richard Brown (2015).

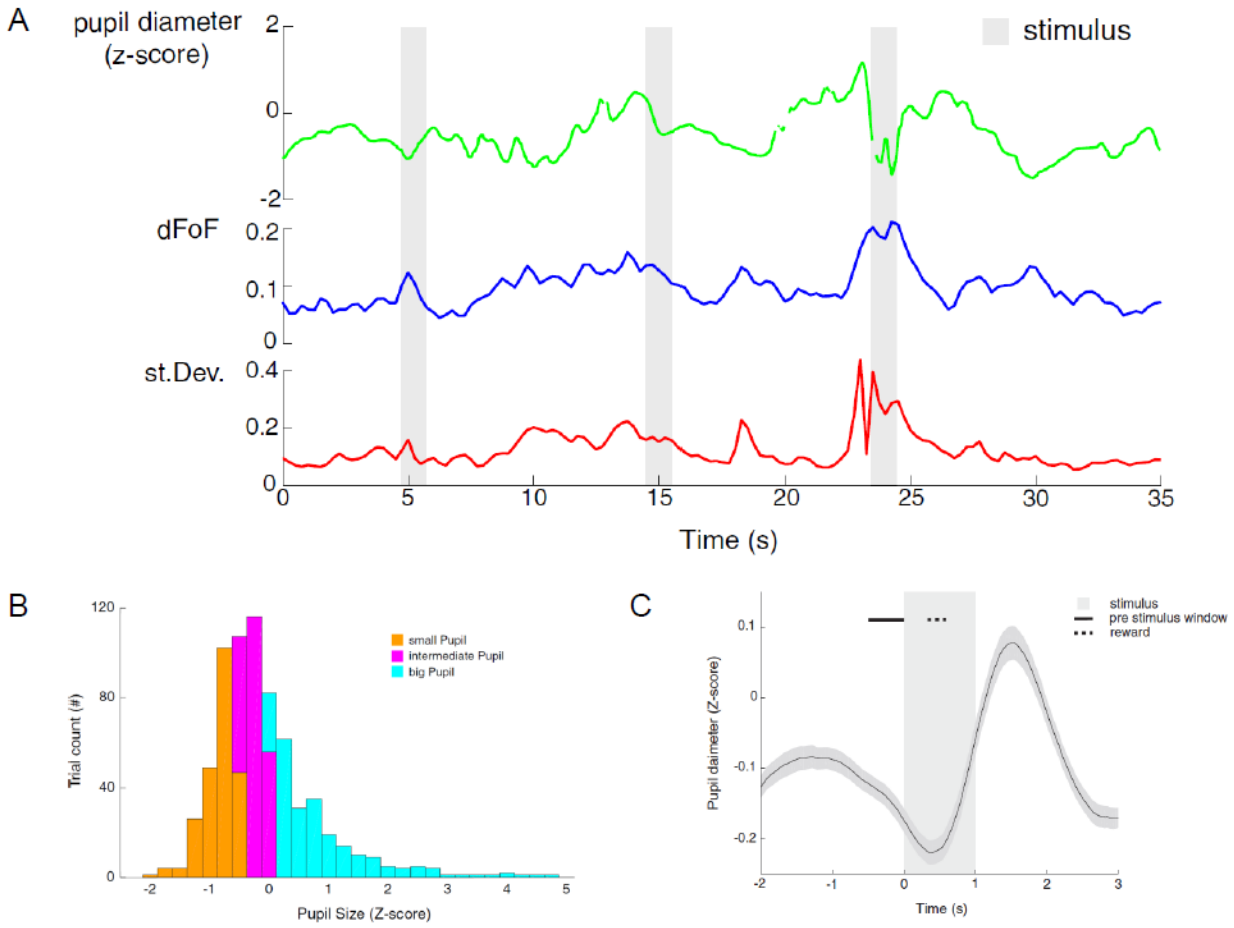

Figure 2 **Pupil interactions with neuronal response and stimulus presentation**
(A) Pupil diameter, average dFoF and average standard deviation over neurons plotted against time. DFoF and standard deviation were averaged over a 0.5s time window with a step size of 0.25s. Gray rectangles indicate stimulus displays. (B) Average pupil size over all trials plotted against time displayed in a window 2 s before to 3 s after stimulus onset. Gray rectangle displays stimulus on and offset. Dotted line shows average reward onset. Black line indicates 0.5 s pre stimulus window. Shaded area plots SEM. (C) Histogram for average pupil size in 0.5 s before stimulus onset for all trials. Different colors indicate quantile split for later analyses.

Ellipse area A was calculated using ellipse side lengths [a b] obtained from equation 3.

$$A = a \times b \times \pi$$

Equation 4

The steps of the Eye-Tracking algorithm have been visualized in figure 1. All traces of pupil area were Z-scored per day before further processing.

Statistical analysis

All statistical analyses were carried out using the MATLAB 'Statistics and Machine Learning Toolbox'. Analyses of neuronal data was based on activity of responsive neurons. To test whether a neuron was responsive, the activity of the neuron during stimulus presentation (to either of the 3 directions) was compared to baseline using a paired t-test. A neuron was considered as responsive when its response to either of the orientations was significantly different from baseline.

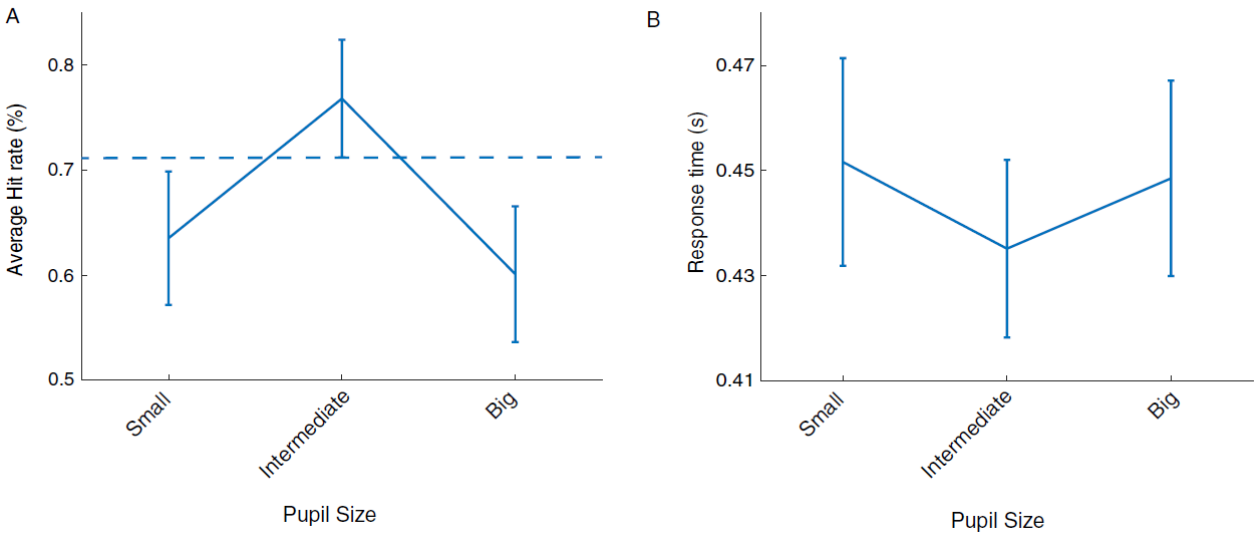

Figure 3 **Behavioral performance at different pupil sizes**
(A) Average hit rate over all trials plotted for all trials split into 3 quantiles of pupil size. Dotted line indicates border of significance for the lower confidence interval of intermediate pupil size. Bars display confidence interval of binomial fit. (B) Average response time plotted for all trials split into 3 quantiles of pupil size. Bars indicate SEM.

Results

Pupil diameter fluctuations are task dependent and affect neuronal response

Pupil diameter was expected to vary rapidly over time. We hypothesized that these fluctuations affect the activity and variability of neuronal response of the primary visual cortex. To observe these interactions, we plotted the trace of the pupil diameter, together with the average activity and the average variability of the neurons' response over time (*Figure 2A*). As expected, neuronal activity and variability reacts to rapid changes in pupil diameter. Notably, these effects are not linearly correlated.

Visual stimulation, due to changes in luminance, and reward delivery are expected to influence pupil diameter. We therefore averaged pupil diameter over visual stimulus trials centered for stimulus presentation (*Figure 2B*). An initial decrease in pupil diameter can be observed after stimulus onset, that can be explained by increases in luminance due to stimulus presentation. The reward onset after 0.3 – 0.5 s is followed by a sharp increase in pupil diameter that drops to baseline about 3 s after stimulus onset.

To classify the state of arousal during the visual detection task, pupil diameter was averaged in a time window of 0.5 s before stimulus onset. These were displayed in a histogram revealing a right skewed normal distribution (*Figure 2C*). The trials were split into 3 quantiles based on pupil diameter, color coded in the histogram. Average pupil sizes in the pre-stimulus window are nearly normal distributed where a number of trials show unusual increases in pupil diameter. Time points of these extreme pupil dilations, although head-fixed, are often accompanied by movement of the animal in the experimental setup.

Optimal task performance observed at intermediate levels of arousal

We used the visual detection task to investigate the neuronal mechanisms of information processing at optimal state of arousal in the primary visual cortex. To test whether the task follows the Yerkes-and-Dodson law of optimal task performance at intermediate arousal levels, we measured task performance in average hit rate and response latency for different pupil sizes.

The pupil diameter was averaged in a 0.5 s window before stimulus onset. All trials were split into 3 groups according to pupil diameter with even groups for small, intermediate and big pupil sizes. The groups were compared for average hit rate and response latency, where average hit rate was found to be highest at intermediate pupil sizes (*Figure 3A*). For statistical analysis a binomial fit for the different groups was calculated. The confidence interval for intermediate pupil size was not overlapping with the confidence intervals of small and big pupil size and therefore considered significantly different. One-way ANOVA for response latency did not yield significant differences ($p = 0.79$) between trials of different pupil sizes (Figure 3B). Optimal task performance is found

to be linked to intermediate level of arousal thereby confirming preceding studies regarding state of

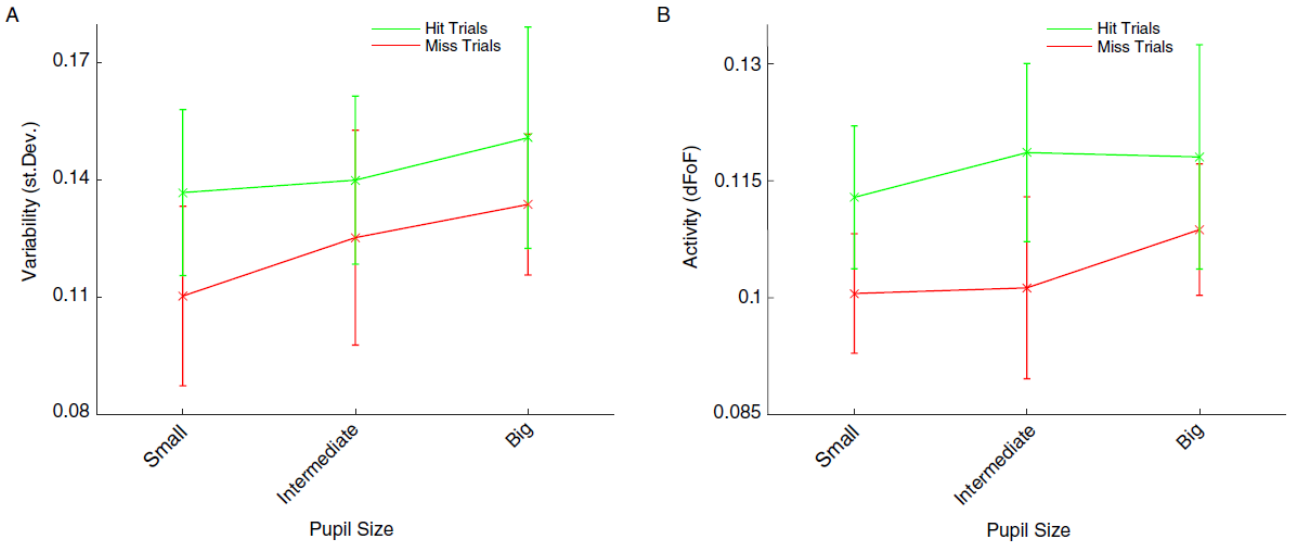

Figure 4 **Evoked activity and variability**
(A) Average dFoF over neurons during stimulus presentation for different quantiles based on average pupil size in a 0.5 s pre stimulus window. Hit trials displayed in green and miss trials displayed in red. Bars indicate SEM. (B) Average variability over neurons during stimulus presentation for different quantiles based on average pupil size in a 0.5 s pre stimulus window. Hit trials displayed in green and miss trials displayed in red. Bars indicate SEM.

arousal and task performance (McGinley et al., 2015b; Yerkes and Dodson, 1908).

Arousal does not affect stimulus evoked activity during a visual detection task

To investigate the effects of the state of arousal on neuronal activity during visual stimulation, all trials were split based on pupil diameter (see *above*) and additionally based on the response of the mouse. We calculated average dFoF over all responsive neurons (see Methods: *Statistical Analyses*) (N_1 = 25/147; N_2 = 23/149) and standard deviation of dFoF over neurons during 1s of stimulus presentation (*Figure 4*). 2-way ANOVA analysis for pupil size and lick response was used for analysis. There was no significant difference of activity for pupil size ($p = 0.82$) and lick response ($p = 0.14$). Analysis for variability did also not yield significant differences between groups for pupil size ($p = 0.73$) or lick response ($p = 0.31$). This stands in contrast to earlier studies that found elevated firing rates and subthreshold potentials in neurons in the primary visual cortices during stimulus presentation (Vinck et al., 2015).

Decorrelation at optimal state improves information encoding

Noise correlations have been shown to influence information encoding in the sensory cortices. There has been evidence, that they can enhance or can be detrimental for information encoding. Even less is known about how noise correlation effect the behavior of the animal. We therefore observed noise correlations during the visual detection task comparing between groups of different pupil sizes and additionally different behavioral responses.

Noise correlations were calculated over trials in a visual detection task over groups, split for pupil and response (see *above*). 2-way ANOVA revealed significant differences between pupil size ($p = 0.003$) and response ($p = 0.04$), there was an increase in noise correlations for trials with a big pupil size compared to intermediate ($p = 0.01$) and small ($p = 0.005$) pupil sizes (*Figure 5*). To compare noise correlations between hit and miss trials at different levels of pupil size, we performed two sample t-tests for every pupil quantile between hit and miss trials. We corrected for multiple comparisons using Bonferroni correction ($p < 0.017$). There were no significant differences at small pupil sizes ($p = 0.50$) or big pupil sizes ($p = 0.99$), however we did find significant results for the intermediate quantile ($p = 0.006$). The differences between hit and miss trials show that noise correlations are a relevant indicator for encoding performance at optimal levels of arousal. These results provide evidence for the hypothesis that a decorrelation of activity is a driving factor for optimal task performance at intermediate arousal levels.

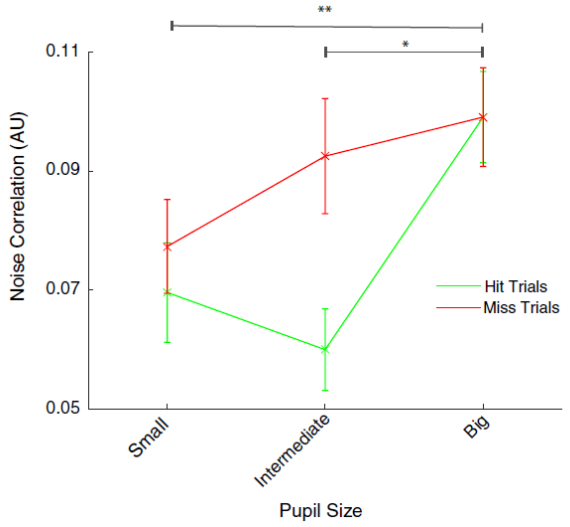

Figure 5 **Noise correlations**
Noise correlations for different quantiles based on average pupil size in a 0.5s pre stimulus window. Hit trials displayed in green and miss trials displayed in red. Bars indicate SEM. *p<0.05, **p<0.01

Arousal interacts with spontaneous activity and average variability over neurons in a U-shaped curve

To examine relationships between spontaneous activity and variability, and pupil size, we calculated average pupil size, average dFoF and average standard deviation in dFoF over neurons in a 0.5 s sliding window with a step size of 0.25 s. Trials were excluded by removing all windows including time points from stimulus onset to 2s after stimulus offset, to remove reward artifacts. The mice were analyzed individually. Only significantly responsive neurons were analyzed (see Methods: *Statistical Analyses*) (N_1 = 25/147; N_2 = 23/149). All windows were split into 10 quantiles according to average pupil size. For each quantile average dFoF and average standard deviation was calculated. One-way ANOVA yielded significance differences between quantiles for both animals for activity ($p_1 = 0.9^{-110}$; $p_2 = 0.2^{-19}$) and variability ($p_1 = 0.5^{-175}$; $p_2 = 0.2^{-39}$). Intermediate quantiles of pupil size were associated with lower spontaneous activity as well as low variability (*Figure 6*). A decrease or increase in pupil size from these levels showed increase in activity and variability. These effects were consistent in both animals except for low levels of pupil size in the first animal, that were not associated with increases in variability. The results on spontaneous activity and variability confirm earlier studies that observed low variability at intermediate levels of arousal (McGinley et al., 2015a). The neuronal correlates paired to different states of arousal imply the existence of cortical states induced by arousal.

Discussion

Recent studies have reported on the interaction between state of arousal and neuronal correlates of primary sensory areas during information encoding, where response and variability in auditory cortex neurons is related in a u-shaped curve with arousal (McGinley et al., 2015b). Our study expands on these results and gives more insight on neuronal mechanisms related to optimal state of arousal. We observed task performance for the visual detection task to be highest at intermediate arousal, quantified in pupillometry, thereby suggesting the optimal state of arousal at intermediate levels. When looking at neuronal response and the variability of the response over neurons in the primary visual cortex layer II/III during the visual detection task, we did not find significant differences between groups for different levels of arousal or response of the mice. Noise correlation were of particular interest in this study as they have not yet been investigated in the context of a sensory detection task that requires a response from the animal. Here we found that an increase in arousal goes paired with an increase in noise correlations. More interestingly we found a significant decrease in noise correlations when comparing hit against miss trials at intermediate state of arousal. This decorrelation was not present in either trials with high or low arousal. As final observation we investigated non stimulus driven activity and variability over neurons for different levels of arousal. We found a u-shaped curve where both activity and variability are low at intermediate level of arousal and a decrease or increase in arousal is accompanied by increase of both activity and variability.

We were able to replicate results of an optimal state of arousal for the visual detection task that has been described in the Yerkes and Dodson law. Based on these results we investigated the average neuronal activity and the variability of the neuronal response during the visual detection task comparing groups of three different pupil sizes. We were not able to replicate results of earlier studies that found increased firing rates in auditory cortex neurons during an auditory detection task at intermediate levels of arousal (McGinley et al., 2015a). A reason for this discrepancy might be the low number of test subjects. This same study also investigated spontaneous firing rates and variability of the neurons in the auditory cortex, finding a u shaped relationship of both to the level of arousal, which we replicated for neurons of the visual cortex. This suggests that the neuronal basis for the relationship of arousal and cortical activity is similar across primary sensory cortices of

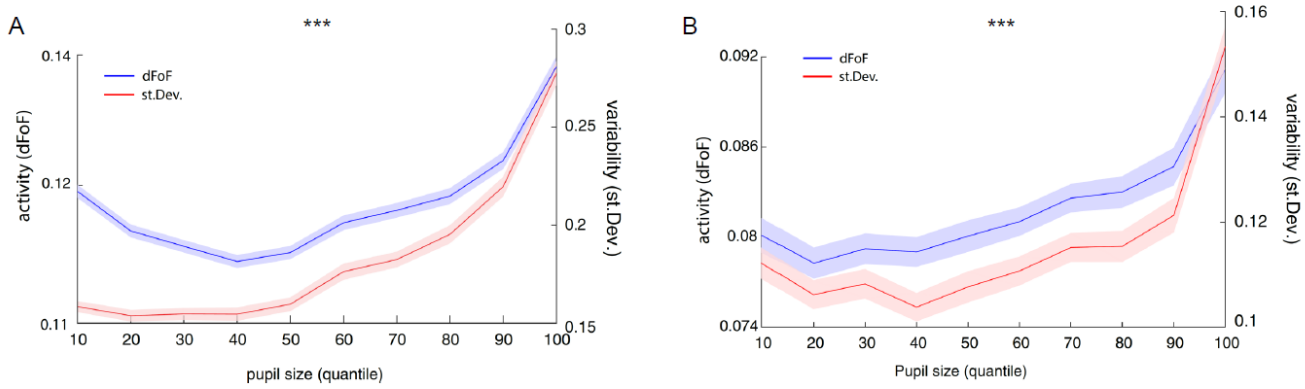

Figure 6 **Spontaneous evoked activity and variability**
A sliding window of 0.5s window width and 0.25 step size was used to calculate average dFoF and standard deviation and average pupil size after excluding trials. Windows were split into 10 quantiles based on average pupil size. Activity and variability were averaged for every quantile over windows for animal 1 (A) and animal 2 (B). ***p<0.001

different modalities. It remains to be seen if these results can be replicated in the cortex of more complex organisms such as the primate brain.

Noise correlations are considered to be of importance in the underlying mechanisms of information coding. Earlier research found decrease of noise correlations at states of high compared to states of lower arousal. Increased arousal, came paired with an improvement in stimuli encoding leading to the conclusion that noise correlations have a detrimental effect on information encoding (McGinley et al., 2015b; Reimer et al., 2014; Vinck et al., 2015). When comparing trials of high arousal against low arousal trials we observed opposite effects, an increase in noise correlations at higher levels of arousal. However, earlier studies did not make a distinction for intermediate levels of arousal or between hit and miss trials. Here we found a decorrelation at optimal state of arousal in hit trials compared to miss trials. Differences in noise correlations for task response of the animal give clear evidence for the hypothesis that a decrease in noise correlations is benefitting for information encoding in the primary visual cortex. Considering that this decorrelation is only observed at the optimal state of arousal suggests that the mechanisms of noise correlations are an important factor for the improvements on sensory processing and the increase in task performance of the animal. Noise correlations are still not fully understood and should therefore be a focus of future research targeting the mechanisms of information coding in the brain.

Our combined results suggest that it is important to consider a broad classification of state of arousal when examining its effects on information coding. This might lead to new insight on the effect of arousal on neuronal correlates, in turn increasing our understanding of network activity in primary sensory areas and information encoding in the cortex. Essential for this goal is the understanding of the pathways of arousal to primary sensory areas. Global cortical circuits have long been investigated and we have a broad understanding of the arousal network. Much less is known about the cellular mechanisms and local circuits of arousal in sensory areas. Different neurotransmitter pathways, mainly the cholinergic, the noradrenergic and the dopaminergic systems have been linked to the mechanisms of arousal (Coull, 1998; Marrocco et al., 1994). How these affect information encoding in primary sensory areas, which types of neurons are targeted in which layers, and how they shape firing patterns are questions for further investigation.

In this study we provide more information on the effects of arousal at optimal state on the cortical processes of sensory processing. The optimal state of arousal has distinct neuronal correlates that imply the benefits of classifying state of arousal into at least 3 distinct groups and distinguishing in the behavioral response of the animal, when investigating the neuronal correlates of state of arousal.

References

Andermann, M.L., Kerlin, A.M., Reid, R.C., 2010. Chronic Cellular Imaging of Mouse Visual Cortex During Operant Behavior and Passive Viewing. Front. Cell. Neurosci. 4. doi:10.3389/fncel.2010.00003

Averbeck, B.B., Latham, P.E., Pouget, A., 2006. Neural correlations, population coding and computation. Nat. Rev. Neurosci. 7, 358–366. doi:10.1038/nrn1888

Beatty, J., 1982. Task-evoked pupillary responses, processing load, and the structure of

processing resources. Psychol. Bull. 91, 276–292. doi:10.1037/0033-2909.91.2.276
Bradley, M.M., Miccoli, L., Escrig, M.A., Lang, P.J., 2008. The pupil as a measure of emotional arousal and autonomic activation. Psychophysiology 45, 602–607. doi:10.1111/j.1469-8986.2008.00654.x
Chen, T.-W., Wardill, T.J., Sun, Y., Pulver, S.R., Renninger, S.L., Baohan, A., Schreiter, E.R., Kerr, R.A., Orger, M.B., Jayaraman, V., Looger, L.L., Svoboda, K., Kim, D.S., 2013. Ultrasensitive fluorescent proteins for imaging neuronal activity. Nature 499, 295–300. doi:10.1038/nature12354
Coull, J.T., 1998. Neural correlates of attention and arousal: insights from electrophysiology, functional neuroimaging and psychopharmacology. Prog. Neurobiol. 55, 343–361. doi:10.1016/S0301-0082(98)00011-2
Ecker, A.S., Berens, P., Cotton, R.J., Subramaniyan, M., Denfield, G.H., Cadwell, C.R., Smirnakis, S.M., Bethge, M., Tolias, A.S., 2014. State Dependence of Noise Correlations in Macaque Primary Visual Cortex. Neuron 82, 235–248. doi:10.1016/j.neuron.2014.02.006
Faisal, A.A., Selen, L.P.J., Wolpert, D.M., 2008. Noise in the nervous system. Nat. Rev. Neurosci. 9, 292–303. doi:10.1038/nrn2258
Franke, F., Fiscella, M., Sevelev, M., Roska, B., Hierlemann, A., Azeredo da Silveira, R., 2016. Structures of Neural Correlation and How They Favor Coding. Neuron 89, 409–422. doi:10.1016/j.neuron.2015.12.037
Goldey, G.J., Roumis, D.K., Glickfeld, L.L., Kerlin, A.M., Reid, R.C., Bonin, V., Schafer, D.P., Andermann, M.L., 2014. Removable cranial windows for long-term imaging in awake mice. Nat. Protoc. 9, 2515–2538. doi:10.1038/nprot.2014.165
Guizar-Sicairos, M., Thurman, S.T., Fienup, J.R., 2008. Efficient subpixel image registration algorithms. Opt. Lett. 33, 156. doi:10.1364/OL.33.000156
Helmchen, F., Denk, W., 2005. Deep tissue two-photon microscopy. Nat. Methods 2, 932–940. doi:10.1038/nmeth818
Li, D., Winfield, D., Parkhurst, D.J., 2005. Starburst: A hybrid algorithm for video-based eye tracking combining feature-based and model-based approaches, in: 2005 IEEE Computer Society Conference on Computer Vision and Pattern Recognition (CVPR'05) - Workshops. Presented at the 2005 IEEE Computer Society Conference on Computer Vision and Pattern Recognition (CVPR'05) - Workshops, pp. 79–79. doi:10.1109/CVPR.2005.531
Loy, G., Zelinsky, A., 2003. Fast radial symmetry for detecting points of interest. IEEE Trans. Pattern Anal. Mach. Intell. 25, 959–973. doi:10.1109/TPAMI.2003.1217601
Marrocco, R.T., Witte, E.A., Davidson, M.C., 1994. Arousal systems. Curr. Opin. Neurobiol. 4, 166–170. doi:10.1016/0959-4388(94)90067-1
McGinley, M.J., David, S.V., McCormick, D.A., 2015a. Cortical Membrane Potential Signature of Optimal States for Sensory Signal Detection. Neuron 87, 179–192. doi:10.1016/j.neuron.2015.05.038
McGinley, M.J., Vinck, M., Reimer, J., Batista-Brito, R., Zagha, E., Cadwell, C.R., Tolias, A.S., Cardin, J.A., McCormick, D.A., 2015b. Waking State: Rapid Variations Modulate Neural and Behavioral Responses. Neuron 87, 1143–1161. doi:10.1016/j.neuron.2015.09.012
Reimer, J., Froudarakis, E., Cadwell, C.R., Yatsenko, D., Denfield, G.H., Tolias, A.S., 2014. Pupil Fluctuations Track Fast Switching of Cortical States during Quiet Wakefulness. Neuron 84, 355–362. doi:10.1016/j.neuron.2014.09.033
Schölvinck, M.L., Saleem, A.B., Benucci, A., Harris, K.D., Carandini, M., 2015. Cortical State Determines Global Variability and Correlations in Visual Cortex. J. Neurosci. 35, 170–178. doi:10.1523/JNEUROSCI.4994-13.2015
Stosiek, C., Garaschuk, O., Holthoff, K., Konnerth, A., 2003. In vivo two-photon calcium imaging of neuronal networks. Proc. Natl. Acad. Sci. 100, 7319–7324. doi:10.1073/pnas.1232232100
Vinck, M., Batista-Brito, R., Knoblich, U., Cardin, J.A., 2015. Arousal and Locomotion Make Distinct Contributions to Cortical Activity Patterns and Visual Encoding. Neuron 86, 740–754. doi:10.1016/j.neuron.2015.03.028
Yerkes, R.M., Dodson, J.D., 1908. The Relation of Strength of Stimulus to Rapidity of Habit-Formation. J. Comp. Neurol. Psychol. 18, 459–482.
Zoccolan, D., Graham, B.J., Cox, D.D., 2010. A self-calibrating, camera-based eye tracker for the recording of rodent eye movements. Decis. Neurosci. 4, 193. doi:10.3389/fnins.2010.00193